

Flow induced pulsations generated in corrugated tubes

S.P.C. Belfroid

TNO Science and Industry, Delft, The Netherlands

R. Swindell

Bureau Veritas, Southampton, United Kingdom

R. Tummers

Eindhoven University of Technology, Eindhoven, The Netherlands

ABSTRACT

Corrugated tubes can produce a tonal noise when used for gas transport, for instance in the case of flexible risers. The whistling sound is generated by shear layer instability due to the boundary layer separation at each corrugation. This whistling is examined by investigating the frequency, amplitude and onset of the pulsations generated by 2" artificially corrugated tubes and cable feeds. Special attention is given to the influence of the geometry of the corrugations and to the influence of the boundary conditions of the tubes. Two distinct modes are measured. One high mode with a typical Strouhal number $Sr=0.35$ and one with a Strouhal number of $Sr=0.1$. The relative length scale for the corrugations to be used in the Strouhal number is a modified gap width, which is the gap width excluding the downstream edge radius. The exact Strouhal number for a corrugation is furthermore dependent on details of the corrugation. The propagation of acoustic waves in the corrugated pipes are subjected to a reduction in the effective speed of sound and an increased damping due the increased pressure drop. The effective speed of sound is reduced due to the added impedance of the corrugation volumes. The damping can be described by adding a frictional pressure drop to the visco-thermal damping. For the visco-thermal damping it was assumed that the corrugated pipe was a smooth pipe. With these assumptions the damping could be matched to the measurements within 10%.

1. INTRODUCTION

Corrugated tubes are extensively used in the process and in the oil and gas industry as they allow for flexible tubes and hoses. The downside of the use of corrugated tubes is that they are known to generate a clear, high amplitude, whistling tone. A Joint Industry Project (JIP), involving ExxonMobil, BP, the UK Health & Safety Executive, TNO and Bureau Veritas, has addressed the technical issues associated with the high amplitude, pressure

pulsations and the associated short term pipe work vibration-induced fatigue issues. The pulsations are generated due to vortex shedding and shear layer instabilities at the corrugations. At each corrugation a boundary layer grows which separates at the upstream edge of the corrugation. This forms an unstable shear layer which can dampen or magnify acoustic flow disturbances. If a coupling occurs with an acoustic field, for instance in the case of an acoustical resonance in the tube, a feedback mechanism occurs where the acoustical field is amplified by the shear layer instabilities and the acoustical field itself magnifies the layer instabilities.

In the JIP by combining actual offshore measurement data; part and full scale test results at low, medium and high pressures; and both theoretical acoustic and flow simulations, the whistling behavior is examined. The whistling behaviour of corrugated tubes has a renewed interest, amongst other things, generated by the occurrence of damages onboard an offshore platform caused by vibrations due to pulsations generated in a corrugated tube (Kopiev, 2005; Kristiansen, 2007; Popescu, 2008), although several authors have been interested in this special topic much earlier (Petrie, 1979; Ziada, 1991). In the project specifically the influence of the detailed geometry of the corrugations on the whistling behavior is investigated. The goal of the project is to come to a prediction tool of the onset of whistling. This also requires a detailed knowledge of the wave propagation properties, such as the damping, in the corrugated tubes. To this end different corrugated tubes have been tested by blowing air through them and measuring amplitudes and frequencies. To determine the damping in the corrugated tubes, separate experiments were done using a siren.

2. EXPERIMENTAL SETUP

The whistling behaviour of the corrugated tubes was examined by flowing air through them and measuring the upstream and downstream dynamic

pressures. The use of multiple transducers allowed for reconstruction of the traveling and standing waves in these sections by using a multi-microphone method. The corrugated tube was set between two (1.605 m) long measurement sections, in which 2 sets of 5 transient pressure transducers were installed. With this setup, waves with frequencies in the range of 31 to 2473 Hz could be reconstructed. By means of a back pressure control valve, the system could be pressurized to operational pressures up to 12 bar(a) (Figure 1).

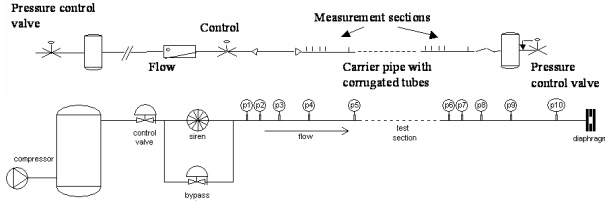


Figure 1: *Experimental setup whistling behaviour (top) and damping (bottom).*

Besides the transient pressure transducers, the static pressure and temperature were measured in the downstream measurement section and the static pressure drop across the measurement section. The mass flow was measured upstream of the flow control valve. These data allow measurement of the flow velocities and the pressure drop across the corrugated tubes.

For corrugated tubes, both commercial tubes (carcasses of real risers and cable feeds) as well as artificial corrugated tubes (PVC) were used. In this paper the results using the artificial corrugated tubes and the cable feeds are presented. Artificial corrugations were used because they allowed for a wide variation in edge radii, depths and widths of the corrugations. An overview of the variations tested in corrugation geometries is given in Table 1 with the geometry parameters defined in Figure 3. Besides symmetric corrugations also non-symmetric corrugations were made to test the influence of installation direction.

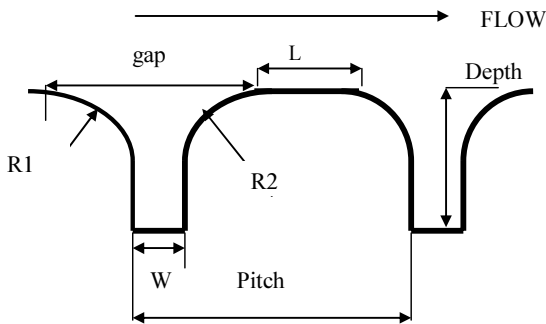


Figure 2: *Definition of corrugation parameters.*

A base experiment consisted of a velocity sweep starting at low velocity up to the maximum possible

flow rate, which at atmospheric conditions was $U=120$ m/s. The total range of Reynolds numbers over which measurements varied was from $Re=1 \cdot 10^4$ up to $1 \cdot 10^6$. At different velocities (step size was approximately 0.4 m/s) a frequency spectrum was measured for each of the 10 pressure transducers. For those frequency peaks with a high coherence between the different measurement positions (per set of 5) a reconstruction was made based on the two-microphone method to reconstruct the upstream and downstream traveling waves. For each velocity this yields the upstream and downstream main frequencies, the amplitude of the pressure pulsations, and the pressure drop over the corrugated tube.

Geometry parameter	Variation
Tube Diameter [mm]	49 for artificial geometries 53, 65 for cable feeds
Pitch [mm]	8 – 16
Gap [mm]	4 – 12
L [mm]	0 – 8
W [mm]	2 – 8
R1 [mm]	0 – 4
R2 [mm]	0 – 4
Depth [mm]	2 – 7
Tube length [m]	≈ 3 for artificial geometries Up to 50 m for cable feeds

Table 1: *Range of parameter variation.*

The same corrugated tubes were used in the damping experiments. In these experiments an active acoustic source (a siren) was used to generate pulsations at defined frequencies at conditions in which the tube was not actively whistling. An experiment consisted of a frequency sweep at a fixed velocity through the corrugated pipe.

By measuring the upstream (p_{up}) and downstream pressures (p_{down}) the transfer ($H(\omega)$) can be obtained and therefore the damping (α) in the corrugated tube, using . To minimize the effect of reflections on the downstream end a multi bore orifice was used to reduce the reflection.

$$\alpha_+ = -\frac{1}{L} \ln \left(\frac{\hat{P}_{down}^+}{\hat{P}_{up}^+} \right) = \frac{-1}{L} \ln |H^+(\omega)| \quad (1)$$

The open/pipe area ratio (a) of the orifice was varied from $a=0.28$, $a=0.19$ and $a=0.1$. Depending on the open area ratio the reflection coefficient could be changed at a given Mach number to less than $|R|<0.1$. Although the reflection at the measured flow rates was minimal still significant reflections on the downstream edge and on the

transitions from the smooth measurement pipe to the corrugated pipe were present. Partly this was due to the change in effective speed of sound in the corrugated tubes. Therefore, the damping coefficients were determined by setting up a transfer matrix of the system of measurement pipes and corrugated pipes and determining the damping required to match the measured pressure amplitudes. The damping was determined at conditions far of any whistling conditions.

3. WHISTLING BEHAVIOUR

At low velocity, below onset, no whistling behaviour is observed. Only the normal flow noise is measured with some acoustical resonances. At a given velocity the whistling starts and a clear tonal noise is generated. As function of the velocity, the corrugated tube generates tones at a specific Strouhal number. That is, the frequency increases linearly with increasing velocity (Figure 3). If the possible axial resonance modes are far apart in frequency, the generated tones can lock in at the distinct resonance frequencies, which result in a more stepwise change in frequency with increasing velocity.

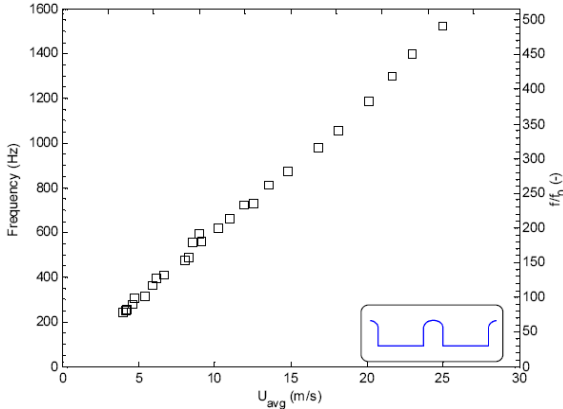


Figure 3: Frequency as function of (average) velocity. f_0 is the first axial resonance frequency of the measurement setup.

It is customary to express the frequency as a Strouhal number (Sr) defined by :

$$Sr = \frac{fL}{U} \quad (2)$$

with f the frequency [Hz], U the mean gas velocity in the tube [m/s] and L a characteristic dimension [m]. It is important to identify the correct length scale. For cavity flow and side branches this is the width of the cavity. For corrugated tubes it has been thought that the pitch would be the determining length scale. We considered three definitions for the length scale: the pitch, the gap width and a

modified gap width ($R1+W$, as defined in Figure 2). This alternative definition is based on the findings of Bruggeman (Bruggeman, 1987; Peters, 2000) where for side branches with rounded edges it was found that the downstream edge radius did not play a role. In Table 2, for a selection of configurations the Strouhal numbers, based on the onset frequency and velocity, are given. It is clear that the pitch is not the correct length scale, as the two geometries 1 and 2 have a similar pitch but a very different Strouhal number. The differences for the definition of the gap or the modified gap are less clear. For the complete dataset the modified gap showed a slightly better resemblance of the Strouhal numbers.

pitch [mm]	gap [mm]	Rup+W [mm]	Sr_pitch [-]	Sr_gap [-]	Sr_Rup+w [-]
12	8	6	0.71	0.47	0.35
12	12	10	0.51	0.51	0.43
8	8	6	0.50	0.50	0.38

Table 2: Strouhal number for selection of configurations. R_{up} is the upstream edge radius.

However, the Strouhal number is not uniquely defined by the adapted gap width. Two sets of Strouhal numbers can be distinguished: one set with ‘high’ Strouhal numbers, around 0.23 - 0.51, and one set with ‘low’ numbers, ranging from 0.04 to 0.2. These two sets of Strouhal numbers form two modes. This is clearly seen in Figure 4, in which the Strouhal number is plotted as function of the dimensionless corrugation volume. This is defined as the ratio of the corrugation volume (V_{cor}) to the volume of the corrugation and the inner pipe ($V_{pitch} = A_{pipe} \cdot l_{pitch}$). For relatively large cavities, the Strouhal number is high. For small corrugations the Strouhal number is low. The higher modes are thought to be associated with flow disturbances due to pressure disturbances. The lower mode is thought to be associated with vortex shedding initiated by acoustic velocity fluctuations. The first is the main mechanism for flow excitation in shallow cavities, while the last is the mechanism encountered in vortex shedding at for instance T-joints (Bruggeman, 1987; Hofmans, 1989).

The reason for the dependence on the cavity geometry is the effective convective velocity of the disturbances in the cavity. For larger corrugations, which often means wider cavities, the disturbances enter the cavity more deeply and therefore, the effective velocity decreases. Of course, the details of the flow behaviour, such as the point of flow separation and streamline paths, are very dependent on the exact geometry of the corrugation such as the edge rounding.

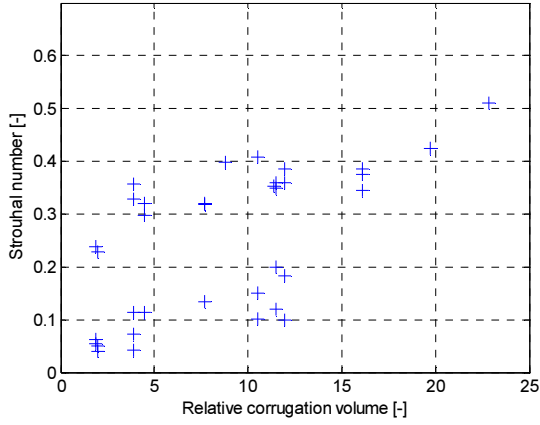


Figure 4: Strouhal number Sr_{Rup+W} as function of relative corrugation volume.

4. DAMPING BEHAVIOUR

The damping coefficient (α) is defined as the imaginary part of the wave number (k) which for a downstream traveling pressure (p) wave results in:

$$p(x) = p(0)e^{-\alpha x} \quad (3)$$

For a smooth pipe the damping is dependent on the ratio of the acoustic boundary layer (δ_{ac}) to the viscous boundary layer (δ_l):

$$\alpha_{eff} = \alpha_0 \quad \text{for } \delta_{ac} \leq \delta_l \quad (4)$$

$$\alpha_{eff} \cong \frac{\delta_{ac}}{\delta_l} \alpha_0 \quad \text{for } \delta_{ac} > \delta_l \quad (5)$$

with α_0 the visco-thermal damping as found by Kirchoff:

$$\alpha_0 = k_0 \frac{\delta_{ac}}{D} \left(1 + \frac{\gamma-1}{\sqrt{Pr}} \right), \quad (6)$$

and for the acoustic boundary layer (δ_{ac}):

$$\delta_{ac} = \sqrt{2\nu/\omega}, \quad (7)$$

with ν the dynamic viscosity [m^2/s], ω the angular frequency [s^{-1}], D the tube diameter [m], γ the isentropic exponent and Pr the Prandtl number [-]. For the test conditions the acoustic boundary layer was almost always thinner than the viscous boundary layer. This leads to a typical damping of $\alpha \approx 0.025 m^{-1}$.

The wave propagation in corrugated tubes is influenced by two effects. The first is a change in effective speed of sound, the second is the damping. The effective speed of sound is reduced by the added impedance of the corrugations. The effective speed of sound (c_{eff}) can, according to Cummings, than be written as (Wright, 2005).

$$c_{eff}^{\pm} = c_0 \frac{k_0}{k^{\pm}} = c_0 \frac{\left(1 \pm M \sqrt{1 + \frac{V_{cor}}{V_{pitch}}} \right)}{\left(\sqrt{1 + \frac{V_{cor}}{V_{pitch}}} \right)} \quad (8)$$

with V_{cor} the corrugation volume [m^3], V_{pitch} the pitch volume which is the tube surface area times the pitch length [m^3] and M the Mach number [-]. The subscript 0 denotes the undisturbed speed of sound. This would lead, for our test corrugated tubes, to changes up to 10%. This change was confirmed by measuring resonance frequencies in the system and comparing them to measurements with a smooth pipe instead of a corrugated pipe. With such changes, reflections at both ends of the corrugated tube are present. This meant that the damping could not be directly measured by measuring the upstream and downstream pressures but that, as discussed, a transfer matrix was required.

The damping in the corrugated pipe is considered to consist of the normal acoustic damping (α_0) and a pressure drop part (α_f). Ingard (Ingard, 1974) has derived a relation between the acoustic damping and pipe resistance:

$$\alpha_{f+} \cong 2 \frac{C_f}{D} M_0, \quad (9)$$

with C_f the Fanning friction coefficient [-], D the pipe diameter [m] and M_0 the Mach number [-]. The pressure drop for a corrugated tube is between 2 to 8 times as high as for a smooth pipe. This means that the friction part of the damping is in the order of $\alpha_f \approx 0.04 m^{-1}$.

4.1 Results

The damping coefficients have been determined for the test corrugated tubes at non-whistling conditions, to avoid the possible sound generation by the cavities. To see the effect of sound generation, an experiment has been done with and without a siren. The results are plotted in Figure 5, where the relative damping coefficients as function of the Strouhal number for a certain test geometry are compared. In the experiments without siren, a Strouhal number of $Sr_{W+R1} = 0.36$ was found. In the experiments with siren a clear dip in the damping, even negative damping, is observed at the same Strouhal number. Although, in the siren experiments the flow rates were such that normally no whistling is observed, clearly, a response of the cavities is measured. The reversed geometry could not be made to whistle in the no siren experiments, and also no dip in the damping is observed in the siren experiments.

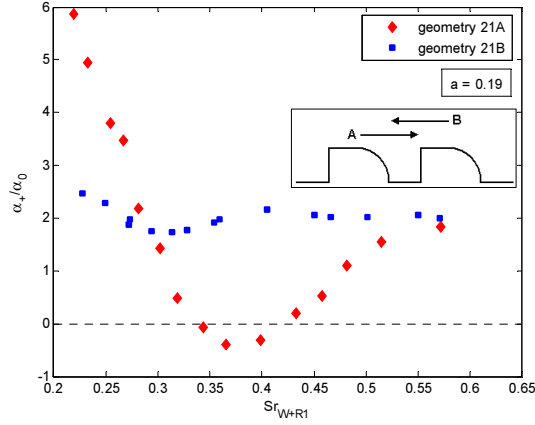


Figure 5: Relative damping coefficient as function of Strouhal number for geometries 21A and 21B.

Geometry	Sr_{W+R1} (frequency)	Sr_{W+R1} (damping)
GEOM10	0.38	0.42
GEOM11	0.36	0.40
GEOM14A	0.33	0.38
GEOM17	0.42	0.36
GEOM18	0.51	0.50
GEOM21A	0.36	0.41

Table 3: Comparison Strouhal numbers based on the active experiments and the damping experiments.

The observed dips in the damping in the siren experiments correspond well with Strouhal numbers found in the no siren experiments (Table 3). A second note on the dip in the damping is that the width of the dip is very broad. A width of $\pm 100\%$ is extremely wide in comparison with the width the Strouhal peaks found of for instance for T-joints $\pm 20\%$ (Hofmans, 1998).

To still determine the damping coefficient, only those experiments at no whistling conditions were considered which means for most configurations low Strouhal numbers ($Sr < 0.1$) and/or high Strouhal numbers ($Sr > 0.6$). In Figure 6 the measured damping, relative to the smooth pipe damping, is plotted as function of the relative pressure drop. In our experiments, the damping measured for the tubes was between 2.5 and 4.5 higher than could be expected for smooth straight pipes. The pressure drop was 1.5-4.5 higher than the pressure drop encountered in a normal straight pipe. The pressure drop in a corrugated pipe consists partly of wall shear at the straight sections and partly of mixing in the corrugations. The mix of these two is very dependent on the details of the geometry and the Reynolds number. Within the

Joint Industry Project a model is developed for the prediction of the pressure drop for corrugated tubes. Within the scope of this paper, however, it is not possible to elaborate on this model.

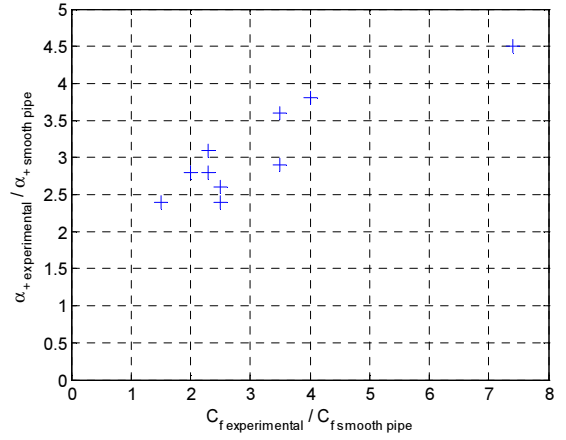


Figure 6: Relative damping coefficient as function of relative friction coefficient (low Strouhal number $Sr < 0.1$).

As discussed, the damping is considered to be partly due to the visco-thermal damping and partly due to the increased pressure drop. At the test conditions the viscous damping is not negligible compared to the pressure drop damping. As Ingard we just added the two together:

$$\alpha_+ = \alpha_{f+} + \alpha_0 \quad (1)$$

For the visco-thermal damping we simply assumed the damping for a straight pipe. Although this is a simplification, this simple addition works very well. In Figure 7 a comparison is made between the experimental and theoretical transfer ratio ($H(\omega)$) as function of the Strouhal number for a certain test geometry. The calculated and measured results agree within 3%. The overall accuracy for also for the other test geometries was 10%.

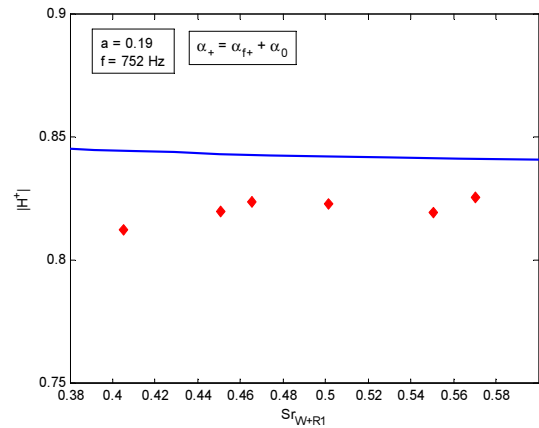


Figure 7: Comparison theoretical and experimental transfer function $|H|$ as function of Strouhal number.

5. CONCLUSION

Depending on the corrugation profile and the termination geometry, some corrugated tubes can generate a whistling tone with amplitudes up to several bars. These pulsations can lead to integrity issues in the up and downstream installations. The whistling behaviour has been experimentally investigated using 2" artificially corrugated tubes and 2" cable conduits. The tubes were found to generate tones at two distinct modes, namely a higher mode with a Strouhal number around $Sr=0.35$ and a lower mode of $Sr=0.1$. The relevant length scale in the Strouhal number is not the pitch but a modified gap width defined as the length of the gap including the upstream edge but excluding the downstream edge radius. This length does not define the Strouhal number uniquely. The Strouhal number for a given geometry is further defined by the cavity volume or the ratio of the upstream edge radius to the gap width.

The propagation of acoustic waves in an scale model has been examined. In the non-whistling region the transfer ratios are measured as function of frequency and flow velocity. A transfer matrix is used to calculate theoretical values taking both the influence of damping and the transitions from a reduced speed of sound into account. The damping coefficient in the test section is calculated using the model developed by Ingard ($\alpha_+ = \alpha_{f+}$), which relates the damping of acoustic waves to the friction of the pipe walls. Using in addition to the friction damping the visco-thermal as found by Kirchhoff for smooth pipes α_0 , resulting in $\alpha_+ = \alpha_0 + \alpha_{f+}$, the measured transfer agree within 10% of the theoretical values. In the whistling region, the damping coefficient showed a large dip at Strouhal numbers corresponding to this found in whistling experiments. The width of the damping dips was very broad compared to Strouhal peaks normally found.

6. ACKNOWLEDGEMENTS

The work discussed in this paper was made possible by the contributions of BP, Bureau Veritas, ExxonMobil, Statoil and the UK Health and Safety Executive. Furthermore, use of the facilities and expertise at the Eindhoven University of Technology was very valuable in particular the help of Prof. A. Hirschberg and J. Bastiaansen.

7. REFERENCES

Belfroid, S.P.C., et al, 2007, Flow induced pulsations caused by corrugated tubes. PVP2007-26503, 2007 ASME PVP Conference San Antonio

Bruggeman J.C., 1987, Flow induced pulsations in pipe systems. PhD thesis Eindhoven University of Technology

Hofmans G.C.J., 1998, Vortex sound in confined flows. PhD thesis Eindhoven University of Technology

Ingard, U, 1974, Sound attenuation in turbulent pipe flow. *J. Acoust. Soc. Am.*, 55: 535-538

Kooijman G, 2007, Acoustic response of shear layers. PhD thesis Eindhoven University of Technology

Kopiev, V.F., 2005, Sound generation, amplification and absorption by air flow through waveguide with periodically corrugated boundary. Forum Acusticum

Kristiansen, U.R., Wiik, G.A., 2006, Experiments on sound generation in corrugated pipes with flow. *J. Acoust. Soc. Am.*, 121:1337-1344

Nakamura, Y., Fukamach N., 1991, Sound generation in corrugated tubes. *Fluid Dynamics Research* 7: 225-261

Naudasher E., Rockwell D., 1994 Flow induced vibrations. 139

Oshkai P., Rockwell D., Pollack M., 2005, Shallow cavity flow tones: transformation from large- to small-scale modes. *J. Sound and Vibration* 280

Peters M.C.A.M., Bokhorst E. van, 2000, Flow-induced pulsations in pipe systems with closed side-branches, impact of flow direction. Proceedings of the Flow-induced vibration 2000 conference, Lucerne, Switzerland.

Petrie A.M., Huntley, I.D. , 1979, The acoustic output produced by a steady airflow through a corrugated duct. *J. of Sound and Vibration*, 70(1): 1-9

Popescu, M., Johansen, S.T., 2008, Acoustic wave propagation in low Mach flow pipe. 46th AIAA Aerospace Sciences Meeting and Exhibit, 2008 Reno Nevada

Swindell R., Belfroid S., 2007, Internal flow induced pulsation in flexible risers. OTC18895

Wright, M.C.M., 2005, Lecture notes on the mathematics of acoustics. Imperial College Press 207-222.

Ziada, S. et al, 1991, Flow induced vibrations in long corrugated pipes. ImechE